

Particle-particle correlations and lifetimes of composite nuclei: New tests for the evaporation model and for statistical equilibration

P. A. DeYoung,⁽¹⁾ C. J. Gelderloos,^(1,2) D. Kortering,⁽¹⁾ J. Sarafa,⁽¹⁾ K. Zienert,⁽¹⁾ M. S. Gordon,^{(2),*}
 B. J. Fineman,⁽²⁾ G. P. Gilfoyle,^{(2),†} X. Lu,^{(2),‡} R. L. McGrath,⁽²⁾ D. M. de Castro Rizzo,^(2,3)
 J. M. Alexander,⁽³⁾ G. Auger,^{(3),§} S. Kox,^{(3),**} L. C. Vaz,⁽³⁾ C. Beck,^{(4),††}
 D. J. Henderson,⁽⁴⁾ D. G. Kovar,⁽⁴⁾ and M. F. Vineyard^{(4),†}

⁽¹⁾Department of Physics, Hope College, Holland, Michigan 49423

⁽²⁾Department of Physics, State University of New York at Stony Brook, Stony Brook, New York 11794

⁽³⁾Department of Chemistry, State University of New York at Stony Brook, Stony Brook, New York 11794

⁽⁴⁾Argonne National Laboratory, Argonne, Illinois 60439

(Received 4 December 1989)

We present data for small-angle particle-particle correlations from the reactions 80, 140, 215, and 250 MeV $^{16}\text{O}+^{27}\text{Al}\rightarrow p-p$ or $p-d$. The main features of these data are anticorrelations for small relative momenta (≤ 25 MeV/c) that strengthen with increasing bombarding energy. Statistical model calculations have been performed to predict the mean lifetimes for each step of evaporative decay, and then simulate the trajectories of the particle pairs and the resulting particle correlations. This simulation accounts very well for the trends of the data and can provide an important new test for the hypothesis of equilibration on which the model is built.

The statistical evaporation model stands as one of the most widely used tools to describe nuclear reaction processes involving composite nuclei with large excitation energies. The working formulas were originally derived by reference to the principle of detailed balance:¹

$$\rho_A w_{ab} = \rho_B w_{ba}^*, \quad (1)$$

where the number of distinguishable states for the initial (final) system is denoted by ρ_A (ρ_B) and the transition rate from a to b (b to a) is w_{ab} (w_{ba}^*). With this postulate the total rate P_v of transitions from a to b is given by the sum

$$P_v = \int w_{ab} = \int \rho_B w_{ba}^* / \rho_A \quad (2)$$

over all paths from a to b , where w_{ba}^* refers to the time reversed transition.

Equation (2) (in various forms) has been implemented in a number of statistical model codes, and observed particle spectra and cross sections are often interpreted in terms of the level densities ρ_B of the residual nuclei and the inverse reaction probabilities w_{ba}^* (or the associated transmission coefficients). Such applications of the model involve only the relative decay rates. However, if one uses a particular model for the level densities of both emitter and residual nuclei ρ_A and ρ_B (generally the Fermi-gas model) and another model for the inverse reaction probabilities w_{ba}^* , then Eq. (2) can predict absolute decay rates P_v or mean lifetimes (P_v^{-1}). A test of these predictions is a test for statistical equilibrium as embodied in Eq. (1). Therefore, such tests can be of fundamental importance for our understanding of the extent of equilibration in nuclear reactions.

The Ericson fluctuation method can provide widths (or lifetimes) in the medium excitation energy regime of overlapping levels.² At still higher energies, measurements of small-angle correlations (SAC) between two evaporated protons have recently been shown to provide lifetime infor-

mation.³ In this work we advance these correlation studies in a number of ways: first, we make measurements over a wide incident energy range 80, 140, 215, and 250 MeV $^{16}\text{O}+^{27}\text{Al}$; second, we present data for both $p-p$ and $p-d$ correlations; third, we compare the correlation data to multistep evaporation calculations.

In a closely related study⁴ we have made symmetry tests of particle correlations for $p-p$, $p-d$, $d-d$, $\alpha-\alpha$, $\alpha-d$, and $d-p$ pairs from 140 MeV $^{16}\text{O}+^{27}\text{Al}$; the results show that the $p-p$, $p-d$, and $d-d$ pairs are consistent with independent particle evaporation and are, therefore, good candidates for tests of evaporation theory. The $\alpha-\alpha$, $\alpha-d$, and $\alpha-p$ pairs do not pass the symmetry test; their correlations are dominated by the decay of particle unstable fragments ^8Be , ^6Li , and ^5Li .

Measurements for 80 and 140 MeV $^{16}\text{O}+^{27}\text{Al}$ were performed at the Stony Brook Linac; and for 215 and 250 MeV ^{16}O at the ATLAS facility of the Argonne National Laboratory. The ^{27}Al targets had areal densities of ≈ 1 mg/cm². Clusters of seven NaI(Tl) detectors were positioned in a hexagonal array as described in Table I. Details concerning the detector characteristics and calibra-

TABLE I. Detector geometry and characteristics. Energy thresholds were 2 and 5 MeV for p and d , respectively, for each NaI(Tl) scintillator. Two seven-member clusters on opposite sides of the beam were used for 80 and 140 MeV, one cluster for 215 and 250 MeV.

Beam energy (MeV)	Flight path (cm)	Mean lab scattering angle	Nearest-neighbor separation	Collimator size (cm)
80	69	45°	4.62°	3.18
140	81	50°	3.91°	3.18
215	124	53.5°	3.00°	3.81
250	124	45°	3.00°	3.81

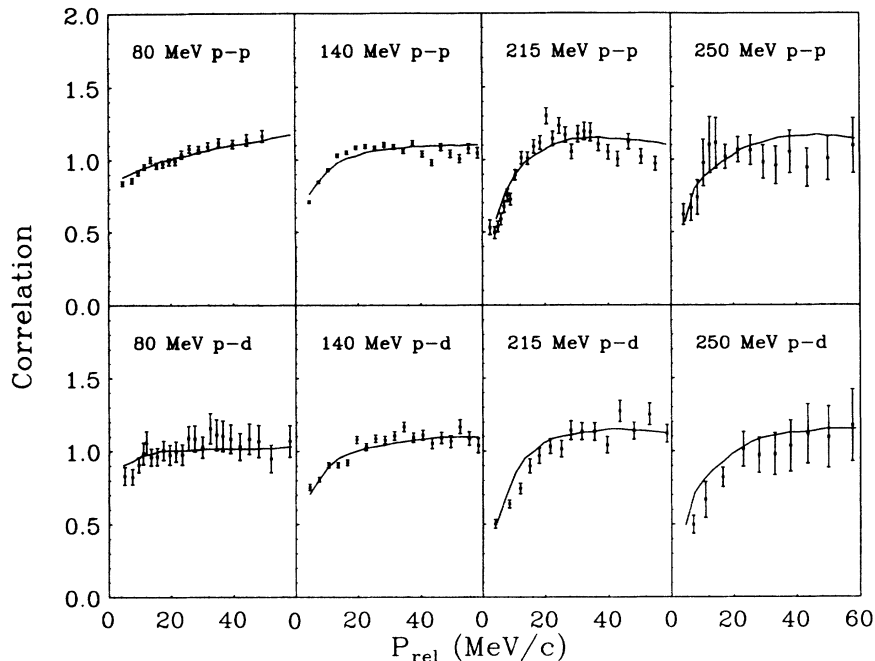


FIG. 1. The p - p and p - d correlations for 80, 140, 215, and 250 MeV incident energy. For both the data and the calculations there is no arbitrary normalization.

tion methods are given elsewhere.³⁻⁶ Small-angle coincidence events (intracluster) were summed over energy and angle and binned in relative momentum P_{rel} to form a spectrum $A(P_{rel})$. A two-particle correlation function is defined as the ratio $A(P_{rel})/B(P_{rel})$ where $B(P_{rel})$ is a reference spectrum free from the correlations of interest. In practice, $B(P_{rel})$ is approximated by false coincidences, constructed either by mixing true coincidence events or from inclusive spectra. As in our earlier work, event mixing has been adopted here and the same number of events is used for both the A and B spectra.

In Fig. 1 we show the observed correlation functions (data points) for p - p and p - d pairs. The calculated curves will be described and discussed below. First, let us note some general features of the data: (a) The major aspect is an anticorrelation for small values of P_{rel} (≤ 25 MeV/ c). (b) The strength of this anticorrelation grows with increasing incident energy. (c) Results from p - p and p - d

pairs are very similar, except for p - p from 215 (and possibly 250) MeV ^{16}O where there is a semblance of a broad peak at ≈ 15 - 35 MeV/ c . In the discussion below we use these results to test predictions of the evaporation model.

To obtain predictions from the statistical model we have used two separate computer programs in conjunction. The first is a Monte Carlo version of the code CASCADE (Ref. 7), which has been modified to calculate the mean lifetime τ [or P_v^{-1} from the equivalent to Eq. (2)] for each particle at each stage (or step) of the evaporation chain. In addition, we sort the output from this CASCADE calculation to obtain the predicted frequency, and the energy spectrum for protons and deuterons at each decay stage. The calculated energy spectra are well described by the function

$$P(E) = (E - V_i)^2 \exp(-E/T_i) \quad (3)$$

with separate values of V_i and T_i for each state i . (These

TABLE II. Stepwise description of proton evaporation (140 MeV $^{16}\text{O} + ^{27}\text{Al}$). For protons we used a Monte Carlo version of the code CASCADE.⁷ This version does not yet treat deuterons so we used the standard CASCADE code to approximate these energy spectra. It also indicates that deuteron emission is essentially confined to the first two steps with equal probability.

Stage (i)	Frequency	$a = A/8$			$a = A/10$			
		V_i (MeV)	T_i (MeV)	τ_i (10^{-22} s)	Frequency	V_i (MeV)	T_i (MeV)	τ_i (10^{-22} s)
1	0.19	1.66	2.96	5.4	0.20	1.66	3.18	3.1
2	0.18	1.65	2.72	7.8	0.19	1.65	2.88	4.5
3	0.17	1.56	2.46	11.3	0.18	1.51	2.62	6.6
4	0.16	1.41	2.20	22.3	0.17	1.38	2.30	12.1
5	0.15	1.26	1.88	1.4×10^2	0.14	1.07	2.24	5.7×10^2
6	0.11	0.17	1.63	2.9×10^4	0.09	-0.35	1.65	4.1×10^4
7	0.04	-0.12	1.07	1.6×10^5	0.02	-0.09	0.94	1.9×10^5

values of V_i and T_i are purely empirical and have no role in the interpretations.) In Table II a set of calculated results (140 MeV $^{16}\text{O} + ^{27}\text{Al}$) is given for two separate values of the level density parameter, $a = A/8$ and $A/10$. Results also have been calculated for the other bombarding energies.

To obtain correlation functions for p - p or p - d pairs, we use a separate simulation program to follow the Coulomb trajectories of each particle.^{3,8} The simulation program is based on the classical idea of evaporative emission. The three basic elements of the model are as follows: (a) Particles are evaporated radially from the surface of a compound nucleus at randomly chosen angles. (b) The particle energies are selected from the distribution functions in Eq. (3). (c) The distribution of time delays between two particles is given by the standard exponential relation characterized by mean times τ_i (see, e.g., Table II). Individual events are generated by a Monte Carlo method. Once the angles of emission, the energies, and the time delay have been chosen, the program calculates the Coulomb trajectory of each, and then tests to see if both particles have hit separate members of a detector pair to give a valid coincidence. For convenience the simulation is done with three "detectors" positioned at the appropriate mean scattering angle (Table I) whose angular separations closely approximate the actual separations of the array.

The input parameters include the numbers needed to define the velocity, charge, and mass of each detected particle, as well as the threshold energy, direction, and opening angle for each detector. The evaporation chain is characterized by "stages" where the energy distribution is described by Eq. (3) with input values of V_i , T_i , and τ_i along with the probability of evaporation for each stage i . Table II gives one example. For each trial event the code proceeds as follows: (1) The particle emission stage for each of the two particles is chosen. (2) The angles of emission are randomly chosen in the angular range where particles can possibly be accepted by the two detectors. (3) The energies are chosen from the appropriate weighting function [Eq. (3)]. (4) The time delay is determined by taking the time difference between the time to emit the second and first particle. For example, if the first particle is emitted in stage i and the second in stage j , then $t_{\text{delay}} = t(i+1) + \dots + t(j)$, where in each step $t(k)$ is chosen from the distribution $t(k) = \exp(-t/\tau_k)$.

In the computation the first particle moves radially during the time taken to give birth to the second. Then the relative velocity and position of the two particles are calculated. The direction of the two-particle center-of-mass (c.m.) velocity is checked to see if it lies in the acceptance range of the detectors. If it does, the asymptotic momenta are found by assuming a hyperbolic Coulomb trajectory in the two-particle c.m. frame. If the two particles hit the two detectors, the relative momentum is calculated and binned. Pseudomomenta are also calculated from mixed events in order to create the reference spectrum used for the correlation function (identical procedure used for data analysis). For 215 and 250 MeV $^{16}\text{O} + ^{27}\text{Al}$ calculations were made for both complete fusion and for incomplete fusion of a ^{12}C at the beam velocity. The calculated

correlation functions turn out to be very similar, and we only give results for complete fusion. For complete fusion the initial lifetime is shorter, but the average number of evaporation steps is greater; these two differences essentially cancel in their effect on the correlation function.

Since quantum mechanics and nuclear interactions are both neglected in this approach, it can have validity only if the particle-particle separation distances are relatively large. In Fig. 2 we show calculated distributions for the time delay between particles and for the distance of closest approach. These distributions are very broad; the average separation distances are hundreds of Fermis and, as shown in Table III, the fraction of events with close encounters ($R_{\text{min}} < 5$ fm) is small (i.e., $< 10\%$) even for 250 MeV $^{16}\text{O} + ^{27}\text{Al}$. Our simple trajectory calculation is thus likely to be adequate for these situations, i.e., for emission times predicted by the statistical evaporation model.

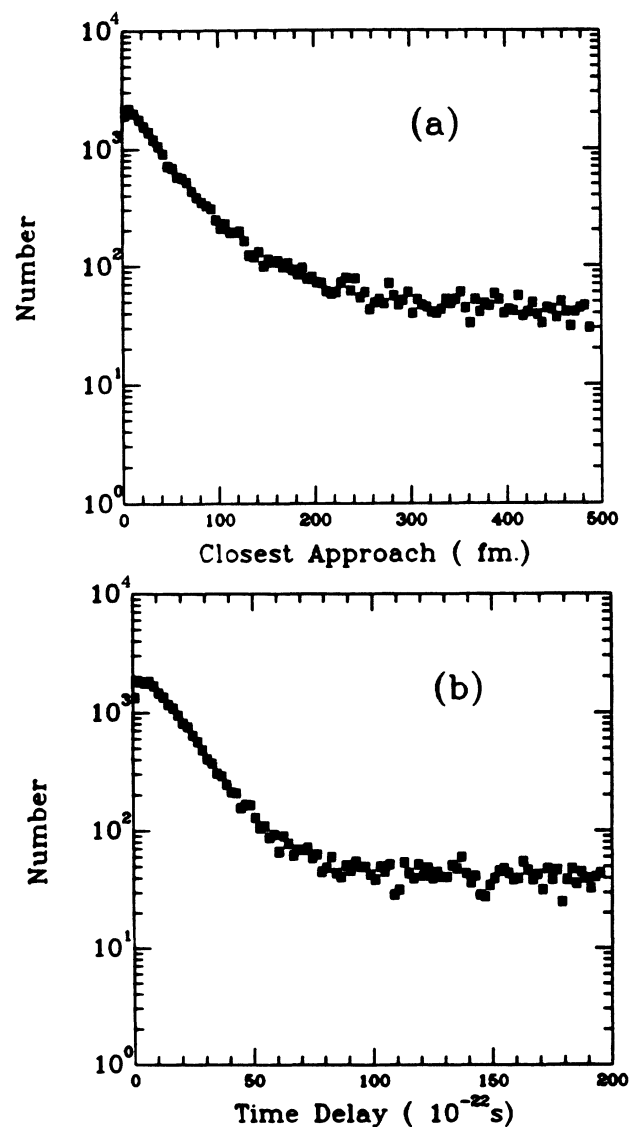


FIG. 2. Simulated distributions for (a) the distance of closest approach and (b) the time delay between emitted particles in the reaction $140 \text{ MeV } ^{16}\text{O} + ^{27}\text{Al} \rightarrow p\text{-}p + X$.

TABLE III. Some average calculated quantities for proton-proton correlations. R_0 is the particle-particle separation at birth, R_{\min} is the particle-particle distance of closest approach for accepted events ($a = A/10$). The particle charge was set to zero so there would not be a correlation in the context of the model for the case given in the third row. Comparison of rows two and three indicates the effect of the Coulomb repulsion.

Energy (MeV)	Fraction ($R_0 < 5$ fm)	Fraction ($R_{\min} < 5$ fm)
80	0.4%	1.6%
140	1.1%	4.1%
140	4.6%	8.4%
215	1.5%	5.1%
250	1.8%	6.5%

Figure 3 shows calculated correlation functions for p - p pairs from the reaction 140 MeV $^{16}\text{O} + ^{27}\text{Al}$; the evaporation model results, e.g., Table II, provided the input for the Monte Carlo trajectory calculations. Calculated lifetimes corresponding to $a = A/10$ are about 60% as long as those for $a = A/8$ (Table II). This results in slightly stronger correlations for $a = A/10$ as shown in Fig. 3(a). In Fig. 4 we show an observed proton spectrum along with calculated spectra for “ a ” values of $A/10$ and $A/8$. The major effect of a change in a is a small slope change at high energies. In this paper our objective is to get a general overview of the expected trend of the correlation functions if statistical equilibration has been achieved. For this purpose we choose $a = A/10$ as a value that is often used and gives a spectral shape at high energies that is similar to our data. We have not attempted to obtain a detailed fit to all the observables as this would take us well beyond the scope of this study.

Now let us return to the correlation functions in Fig. 1; the solid curves were calculated as described above. It seems that these calculations can account for the trends of the data, however, there tends to be a small underestimate of the strength of the observed correlations. In addition, the evaporation model (for independent protons) does not reproduce the semblance of a broad peak for $P_{\text{rel}} \approx 15$ – 35 MeV/ c in the p - p correlations at the higher incident energies. Otherwise, the trends of the small-angle correlation data are generally consistent with the pattern of lifetimes predicted by use of the equilibrium theory. For the data in Fig. 1 the relevant range of nuclear temperatures spans a wide range, i.e. from ≈ 1 MeV (for the final emission step) to ≈ 5 MeV (for the temperature of the initial composite nucleus formed by 250 MeV $^{16}\text{O} + ^{27}\text{Al}$). The correlation is significantly damped by detection of particles emitted late in the cooling process as illustrated in Fig. 3(b), where the simulation for the full chain is compared to one where emission is assumed to occur in the first two stages.

The deviations between calculations and data in Fig. 1 might indicate that the actual nuclear lifetimes are somewhat shorter than those predicted. However, we do not wish to draw such a conclusion until our simulation model has been further refined. For example, the evaporation model predicts a distribution of mean lifetimes for each

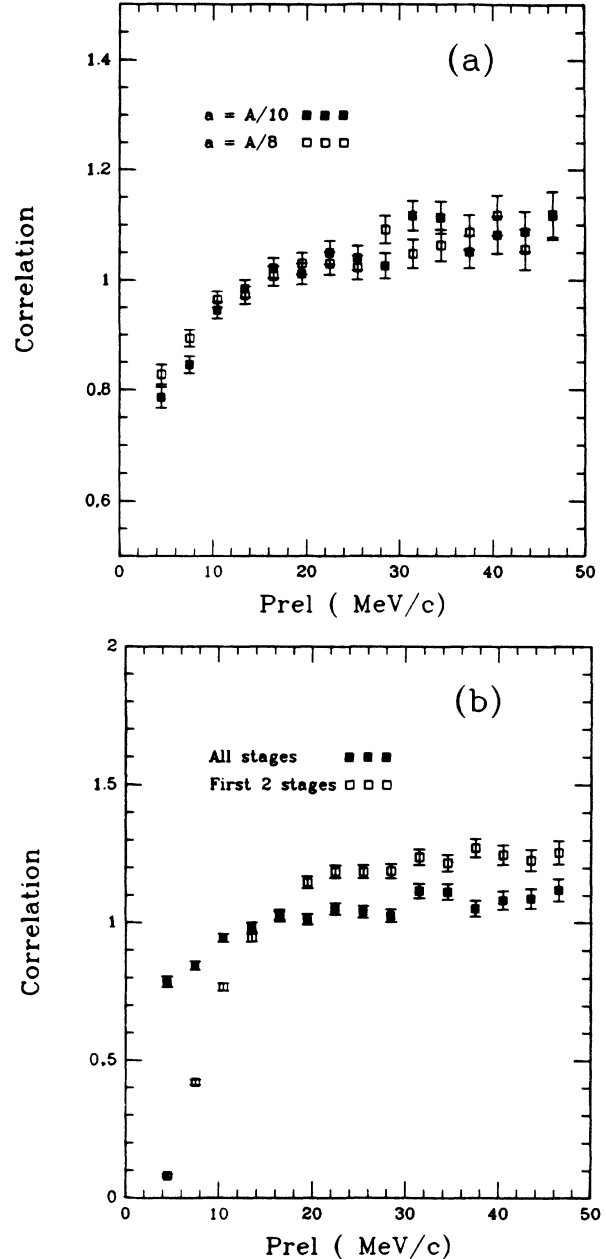


FIG. 3. Simulated p - p correlations for 140 MeV $^{16}\text{O} + ^{27}\text{Al}$ using the statistical model. In (a) two choices of the level density parameter a are compared. See Table II for the input to the calculation. The simulations have 70 000 events, and the error bars suggest the accuracy with which the smooth lines in Fig. 1 were drawn. (b) The same simulation with $a = A/10$ is compared to one where emission is allowed only in the first two stages of the cooling process.

step, only the average of which has been used here. Preliminary estimates indicate somewhat stronger correlations when these distributions are included. These, and other effects, will be considered in further developments of the reaction simulations.

The correlations of other particle species, e.g., d - α or α - α , exhibit peaks associated with well-known nuclear resonances. In a separate paper⁴ we show, at least for 140

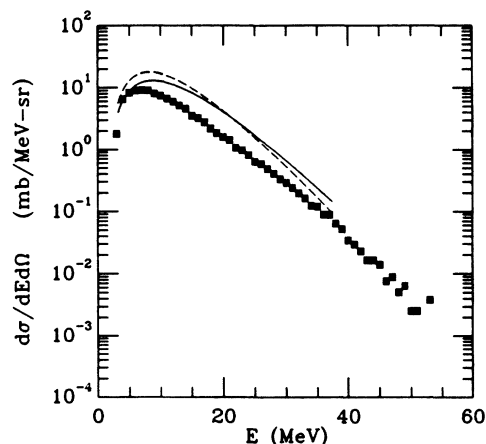


FIG. 4. Inclusive laboratory spectra for protons at $\theta_{\text{lab}} = 50^\circ$ (140 MeV $^{16}\text{O} + ^{27}\text{Al}$). Solid and dashed lines show statistical model calculations (CASCADE) using $a = A/10$ and $A/8$, respectively.

MeV $^{16}\text{O} + ^{27}\text{Al}$, that these cases are strongly influenced by sequential decay, and hence carry no direct information about evaporation lifetimes. The small mismatch between the calculated curves and the 215 and 250 MeV p - p correlation data may be related to our neglect of the nuclear force, and, in particular to ^2He formation and decay. Bernstein *et al.*,⁹ in a correlation study of the same reaction, have shown that this can be an important effect at

more forward angles and at 400 MeV incident energy. In general the relative influence of sequential ^2He decay compared to independent proton emission is expected to increase with increasing excitation energy in an evaporation model.⁹

To summarize, we have presented p - p and p - d correlations in an energy regime where particle evaporation from a compound nucleus is important. The trends of the correlation patterns have been accounted for by an approach that uses standard statistical model parameters to give particle energy distributions and lifetimes together with final-state interactions from the long-range Coulomb force. In this study of p - p and p - d pairs, the average time interval between emissions is rather long because of the many emission steps involved. In future work it should be possible to choose gating conditions that will emphasize the short delay times between the first few emission steps. It seems to us that the small-angle correlation technique constitutes a major new test for statistical equilibration and a tool for the study of the statistical properties of hot nuclei.

We thank A. Elmaani, T. Ethvignot, and M. Herman for their help. The accelerator staffs at Stony Brook and at Argonne were very helpful and efficient. This research was supported by the United States National Science Foundation and the Department of Energy, the William and Flora Hewlett Foundation of Research Corporation, and the Centre National de la Recherche Scientifique of France.

*Present address: IBM General Technology Division, E. Fishkill, NY 12533.

†Present address: Department of Physics, University of Richmond, Richmond, VA 23173.

‡Permanent address: Institute of Atomic Energy, Beijing, China.

§Permanent address: Grand Accélérateur National d'Ions Lourds, Boîte Postale 5027, 14021 Caen, CEDEX, France.

**Permanent address: Institut des Sciences Nucleaires, 53 avenue des Martyrs, 38026 Grenoble CEDEX, France.

††Permanent address: Centre Nucleaire, Boîte Postale 20, 67037 Strasbourg CEDEX, France.

¹T. Ericson, *Adv. Phys.* **9**, 423 (1960), and references therein.

²T. Ericson, *Ann. Phys. (N.Y.)* **23**, 390 (1966).

³P. A. DeYoung, M. S. Gordon, Xiu qin Lu, R. L. McGrath, J. M. Alexander, D. M. de Castro Rizzo, and L. C. Vaz, *Phys. Rev. C* **39**, 128 (1989).

⁴M. S. Gordon, P. A. DeYoung, X. Lu, R. L. McGrath, J. M. Alexander, D. M. de Castro Rizzo, and G. P. Gilfoyle (un-

published).

⁵P. A. DeYoung, R. L. McGrath, and W. F. Piel, Jr., *Nucl. Instrum. Methods* **226**, 555 (1984).

⁶M. S. Gordon, Ph.D. thesis, State University of New York at Stony Brook, 1989 (unpublished).

⁷M. Herman, University of Rochester Nuclear Structure Research Laboratory Report No. UR-NSRL-318 (unpublished); and (private communication); F. Puhlhofer, *Nucl. Phys. A* **280**, 267 (1977).

⁸R. L. McGrath, A. Caraley, B. Fineman, M. S. Gordon, J. M. Alexander, A. Elmaani, and P. A. DeYoung, Annual Report of the Nuclear Structure Laboratory, SUNY at Stony Brook, 1979 (unpublished), p. 89; R. L. McGrath, A. Elmaani, J. M. Alexander, P. A. DeYoung, T. Ethvignot, M. S. Gordon, and E. Renshaw, *Comput. Phys. Commun.* (to be published).

⁹M. A. Bernstein, W. A. Friedman, W. G. Lynch, C. B. Chitwood, D. J. Fields, C. K. Gelbke, M. B. Tsang, T. C. Awes, R. L. Ferguson, F. E. Obenshain, F. Plasil, R. L. Robinson, and G. R. Young, *Phys. Rev. Lett.* **54**, 402 (1985).